Epitaxial *a*-axis and *c*-axis oriented growth of YNi_2B_2C thin films

2001 J. Phys.: Condens. Matter 13 L355

(http://iopscience.iop.org/0953-8984/13/18/103)

INSTITUTE OF PHYSICS PUBLISHING JOURNAL OF PHYSICS: CONDENSED MATTER

J. Phys.: Condens. Matter **13** (2001) L355–L360 www.iop.org/Journals/cm PII: S0953-8984(01)21798-6

LETTER TO THE EDITOR

Epitaxial *a*-axis and *c*-axis oriented growth of YNi_2B_2C thin films

S C Wimbush, K Häse, L Schultz and B Holzapfel

IFW Dresden, PO Box 270016, 01171 Dresden, Germany

E-mail: s.c.wimbush@ifw-dresden.de

Received 9 February 2001, in final form 16 March 2001

Abstract

Epitaxial thin films of the superconducting borocarbide compound YNi_2B_2C have been grown on single-crystal MgO substrates using pulsed laser deposition. For deposition temperatures around 650 °C, *a*-axis oriented films with a dual in-plane orientation are obtained, while at around 750 °C, *c*-axis oriented epitaxial growth occurs. In both cases, the out-of-plane texture has a full width at half-maximum (FWHM) of typically 3°, while the in-plane texture has a typical FWHM of 5° in the *a*-axis oriented case and 2.5° in the *c*-axis oriented case. The electrical characteristics of the films reveal that the quality of the *a*-axis oriented sample is lower than that of the *c*-axis oriented one, which is comparable to that of available single crystals. Superconducting transition temperatures of 12.3 K and 14.5 K were measured for the *a*-axis and *c*-axis oriented samples, respectively, while their residual resistance ratios were found to be 3 and 9.

The intermetallic series of rare-earth nickel borocarbides, RNi_2B_2C, has been extensively studied due to the interplay of magnetic ordering and superconductivity that exists in various combinations throughout the series. The non-magnetic members of the series were initially classified as conventional BCS-type superconductors [1] having a moderate to strong electron–phonon coupling constant [2], and a large density of states at the Fermi level [3], close to that of the traditional A-15 superconductors. With the availability in recent years of high-quality single-crystal samples, the situation changed somewhat as some properties of YNi_2B_2C and $LuNi_2B_2C$ were observed which might be interpreted as indications of unconventional (*d*-wave) superconductivity [4], for example an anisotropy of the upper critical field within the basal plane of $LuNi_2B_2C$, a quadratic flux line lattice at high magnetic fields and an unconventional behaviour of the specific heat. (For an overview see [5] and references therein.) The availability of epitaxial thin films of the non-magnetic borocarbides would enable phase-sensitive tunnelling experiments to be performed, which could help to clarify the question of unconventional superconductivity in the borocarbides. Borocarbide thin films have been prepared by several groups, using both sputtering [6, 7] and pulsed laser deposition [8, 9], the most-reported results being obtained on *c*-axis oriented fibre-textured

films. But phase-sensitive experiments, such as those performed on high-T_C thin films [10], can only be performed on samples having good in-plane, as well as out-of-plane, texture. Furthermore, a-axis oriented films would enable a variety of experiments probing the anisotropic characteristics of the series, hitherto impossible with the available thin-film and single-crystal samples. Recently, a first indication of epitaxial c-axis growth in borocarbide films prepared by laser deposition has been presented [11], but no single epitaxial relationship was obtained. Here, the results are presented of a technique that enables the growth of both a-axis and c-axis oriented epitaxial borocarbide thin films.

For this work, thin films of YNi_2B_2C were deposited in an ultrahigh-vacuum (base pressure $<10^{-9}$ mbar) pulsed laser deposition apparatus, described fully elsewhere [8]. A polycrystalline YNi_2B_2C target, prepared by arc melting, was fired upon at 30 Hz with an energy density $\sim$5 J cm^{-2}, leading to a deposition rate of around 2 nm per second. An MgO(001) substrate was held 2 cm above the target, and heated during deposition to a range of temperatures, T_D, monitored via a thermocouple mounted at the rear of the heater. Only the deposition temperature was varied in the films presented here; all other deposition parameters remained constant.

Structural analysis of the films was performed using x-ray θ–2θ measurements, followed by in-plane texture determination (pole figure measurement). The superconducting transition temperature, T_C, was measured inductively using an alternating magnetic field shielding technique. On selected films, resistivity measurements were made using a four-point probe across a photolithographically patterned bridge.

A steady increase in T_C with increasing deposition temperature was observed (figure 1) as the formation of the 1221 borocarbide phase improved, evidenced by a sharpening of the borocarbide peaks on the x-ray diffraction patterns. Towards the higher temperatures, the T_C of the films approaches the bulk value of 15.5 K, although the ultimate deposition temperature is limited by the tendency for the films deposited at temperatures higher than 775 °C to fail to adhere well to the substrate, resulting in gaps appearing in the film. In the case of the film deposited at 850 °C, this problem is already very severe, with much of the film flaking away gradually after deposition, making extensive measurements difficult.

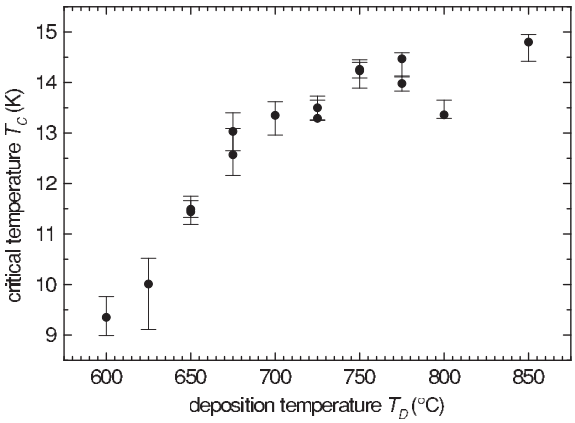

Figure 1. The dependence of the inductively measured critical temperature of YNi_2B_2C films on the deposition temperature. The bars indicate the transition width (90%–10%). Repeated measurements at some temperatures are for multiple films.

θ–2θ x-ray scans of the low-temperature films reveal a dominant (200) borocarbide peak, which gradually diminishes in intensity and is replaced by a set of (00l) peaks as the deposition temperature is increased (figure 2). The former, a-axis oriented films are found to grow best at temperatures around 650 °C, while the latter c-axis oriented films are strongest at 750 °C. Scanning electron microscope images of the sample surface (figure 3) show different grain

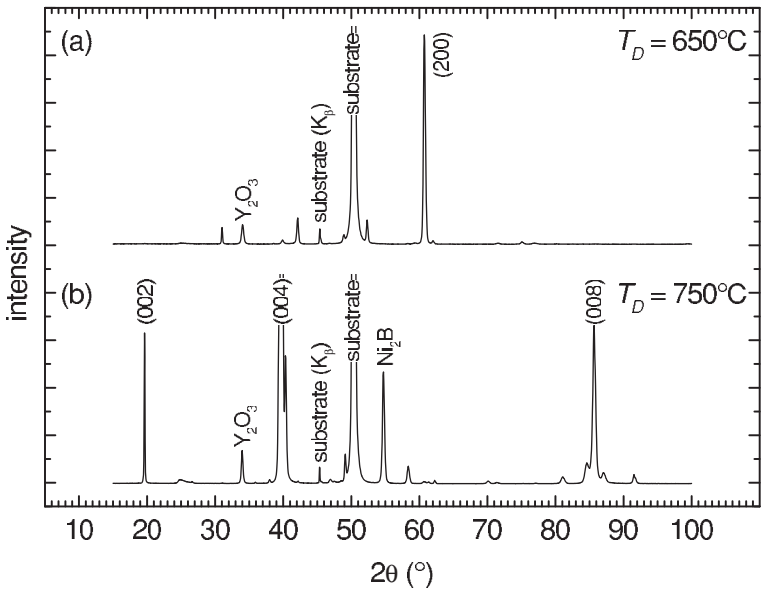

Figure 2. θ–2θ x-ray (Co Kα) diffraction patterns of (a) a-axis and (b) c-axis oriented films with major peaks labelled. Indexed peaks belong to YNi_2B_2C.

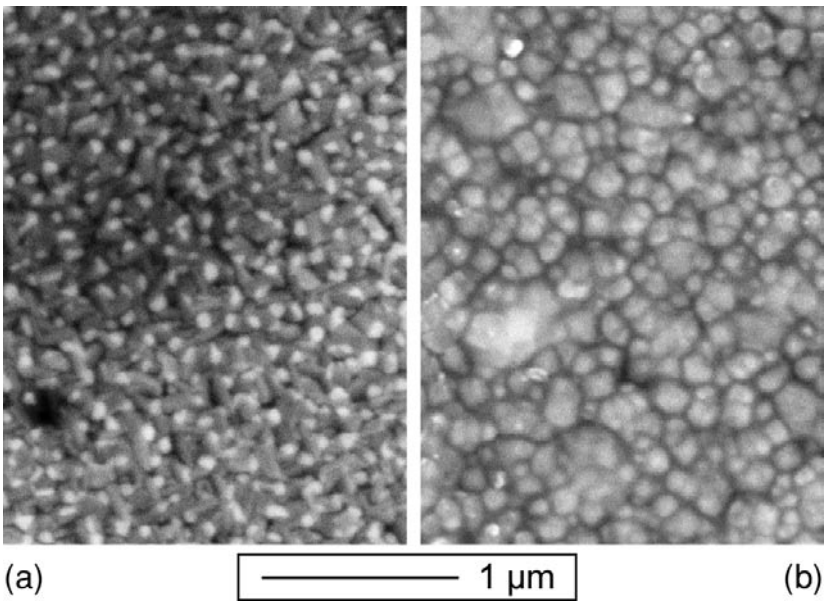

Figure 3. Scanning electron microscope images of the surface of (a) an a-axis and (b) a c-axis oriented film.

structures in the two cases, with larger, more distinct borocarbide grains being formed at the higher temperature. The typically 700 nm thick films exhibit an rms surface roughness across a 5×5 μm area of 9 nm (a-axis oriented) compared with 25 nm (c-axis oriented). The smoothness of the a-axis oriented films also makes obtaining a clear SEM image difficult.

This transition between a-axis and c-axis oriented structures is supported by the x-ray texture measurements of the (211) peak of the aforementioned two films (figures 4(a) and 4(b)). Also shown is the measurement obtained from the best-textured film observed to date (figure 4(c)). The (211) peaks are found at $\psi = 51^\circ$ in the case of an a-axis orientation, and at $\psi = 65^\circ$ for a c-axis orientation. On figure 4(b), in addition to the c-axis texture clearly visible on figure 4(c), and the very faint remainder of the a-axis texture seen in figure 4(a), the (111) peak of the cubic MgO substrate can also be seen at $\psi = 55^\circ$, and this allows the determination of the epitaxy relations for the films. The a-axis oriented film is seen to grow in the two equivalent orientations on the substrate $YNi_2B_2C(100)[001] \parallel MgO(001)[100]$ and [010], while the c-axis oriented film grows in a single orientation rotated by 45° with respect to the cube-on-cube texture of the a-axis: $YNi_2B_2C(001)[110] \parallel MgO(001)[100]$.

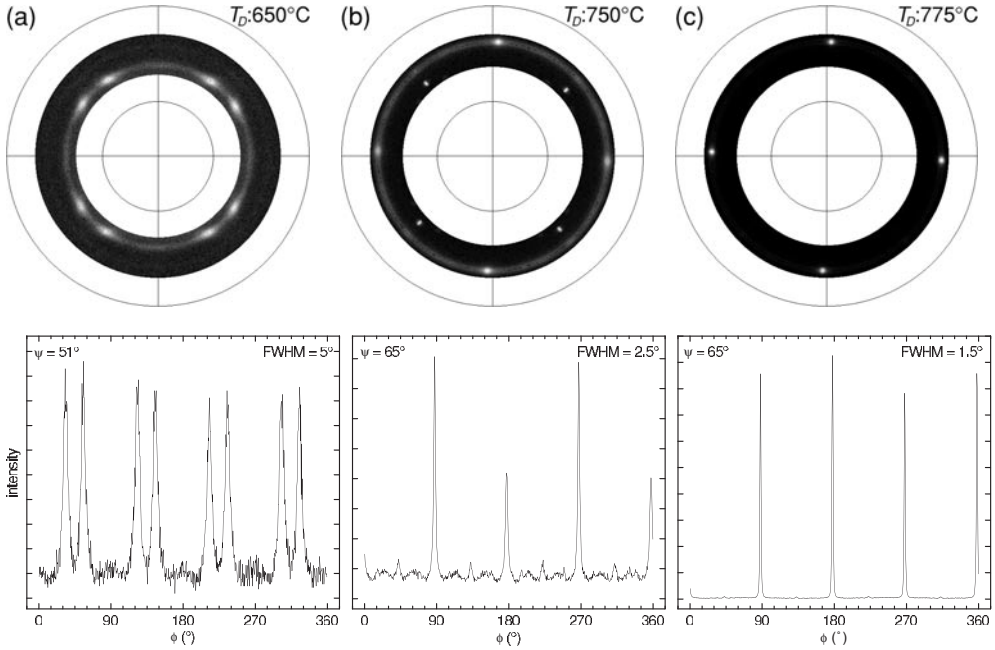

Figure 4. X-ray texture measurements of (a) a-axis and ((b), (c)) c-axis oriented films. The upper images are the pole figures, as measured for each sample. Below these, scans of the intensity variation in the φ-direction have been extracted at ψ-angles of 51° or 65°, corresponding to the expected peak location for a-axis and c-axis orientations, respectively.

Below the pole figures, φ-scans are extracted at the appropriate angle for the orientation of interest. These φ-scans allow a quantitative statement of the degree of in-plane texture. The a-axis oriented films show a typical in-plane full width at half-maximum (FWHM) of around 5°, while for the c-axis oriented films it is typically 2.5°, and it has been observed (figure 4(c)) to be as good as 1.5°. In all cases, the out-of-plane FWHM is around 3°.

The electrical properties of the a-axis and c-axis oriented films under discussion were also examined. Their resistance was measured, from room temperature down to a few kelvins (figure 5), and the zero-resistivity temperatures of the superconducting transitions thus obtained, $T_C = 11.9$ K (transition width $\Delta T_C = 0.9$ K) for the a-axis oriented film and $T_C = 14.1$ K ($\Delta T_C = 0.6$ K) for the c-axis oriented film, are comparable with the results already seen inductively. The residual resistivity ratios of the two films, 3 (a-axis oriented) and 9 (c-axis oriented), provide an indication that at the lower deposition temperature of the

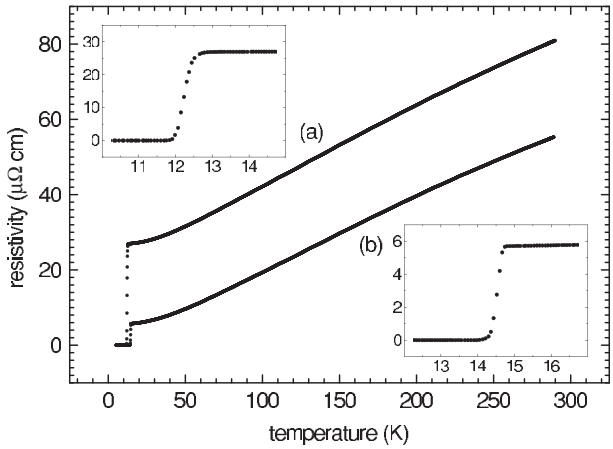

Figure 5. Resistivity versus temperature curves for the (a) *a*-axis and (b) *c*-axis oriented films. The insets show in detail the superconducting transitions.

a-axis oriented films, a higher density of growth defects occurs than at the higher deposition temperature of the *c*-axis oriented films, with both values lying below those obtained from good single-crystal samples. Similarly, the absolute resistivity at the onset of the superconducting transition, 27 $\mu\Omega$ cm for the *a*-axis oriented film and 5.7 $\mu\Omega$ cm for the *c*-axis oriented film, shows moderate agreement with single-crystal values for the *c*-axis oriented film, but is very much higher in the *a*-axis oriented case. The upper critical fields of the two samples, measured at 3 K with the field applied perpendicular to the plane of the film, were found to be around 5 T in both cases. For the *c*-axis oriented film, an anisotropy in the upper critical field was observed when the field was applied instead in the plane of the film, increasing the value to nearly 6 T. No such anisotropy was observed in the *a*-axis oriented film.

In summary, superconducting thin films of YNi_2B_2C have been prepared epitaxially by pulsed laser deposition. By varying the substrate temperature during deposition, it has been found possible to influence the growth of the film such that either an *a*-axis (low temperatures) or a *c*-axis (high temperatures) orientation of the film with respect to the substrate is obtained, in all cases with a high degree of in-plane as well as out-of-plane orientation. Electrical measurements have shown the *c*-axis oriented films to be comparable in quality to available single-crystal samples; the *a*-axis oriented films, due to their lower deposition temperature, suffer from a somewhat higher defect concentration.

This work was supported by the Deutsche Forschungsgemeinschaft as part of SFB463, 'Rare earth transition metal compounds: structure, magnetism and transport'.

References

[1] Mattheiss L F 1994 *Phys. Rev.* B **49** 13 279–82
[2] Bommeli F, Degiorgi L, Wachter P, Cho B K, Canfield P C, Chau R and Maple M B 1997 *Phys. Rev. Lett.* **78** 547–50
[3] Pickett W E and Singh D J 1994 *Phys. Rev. Lett.* **72** 3702–5
[4] Wang G and Maki K 1998 *Phys. Rev.* B **58** 6493–6
[5] Drechsler S L, Shulga S V, Müller K H, Fuchs G, Freudenberger J, Behr G, Eschrig H, Schultz L, Golden M S, Vonlips H, Fink J, Narozhnyi V N, Rosner H, Zahn P, Gladun A, Lipp D, Kreyssig A, Löwenhaupt M, Köpernik K, Winzer K and Krug K 1999 *Physica* C **317–318** 117–26

[6] Arisawa S, Hatano T, Hirata K, Mochiku T, Kitaguchi H, Fujii H, Kumakura H, Kadowaki K, Nakamura K and Togano K 1994 *Appl. Phys. Lett.* **65** 1299–301
[7] Andreone A, Iavarone M, Vaglio R, Manini P and Cogliati E 1996 *Appl. Phys. Lett.* **69** 118–20
[8] Häse K, Holzapfel B and Schultz L 1997 *Physica* C **28** 28–32
[9] Cimberle M R, Ferdeghini C, Guasconi P, Marre D, Putti M, Siri A S, Canepa F, Manfrinetti P and Palenzona A 1997 *Physica* C **282–287** 573–4
[10] Tsuei C C, Kirtley J R, Ren Z F, Wang J H, Raffy H and Li Z Z 1997 *Nature* **387** 481–3
[11] Grassano G, Cimberle M R, Ferdeghini C, Iavarone M, Di Capua R, Vaglio R and Canepa F 2000 *Physica* C **341–348** 757–8